New architectures from the self-assembly of $M^{II}SO_4$ salts with bis(4-pyridyl) ligands. The first case of polycatenation involving three distinct sets of 2D polymeric (4,4)-layers parallel to a common axis

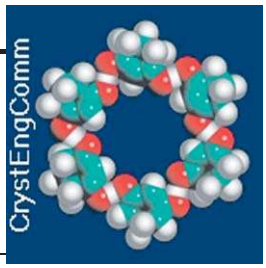

Paper

Lucia Carlucci, Gianfranco Ciani,* Davide M. Proserpio and Silvia Rizzato

Dipartimento di Chimica Strutturale e Stereochimica Inorganica, Università di Milano, via G. Venezian 21, 20133 Milano, Italy. E-mail: davide.proserpio@istm.cnr.it

Received 16th April 2003, Accepted 12th May 2003
First published as an Advance Article on the web 20th May 2003

New network structures and topologies have been obtained from the reactions of different metal(II) sulfates with three bis(4-pyridyl) spacer ligands, that illustrate the influence of the SO_4^{2-} anions in the self-assembly of polymeric coordination architectures. The products include $[Fe(bpp)_2(SO_4)]$ [bpp = bis(4-pyridyl)propane] (**1**), $[Cd(bpethy)(SO_4)]$ [bpethy = bis(4-pyridyl)ethyne] (**2**), $[Cu(bpe)(SO_4)(H_2O)]\cdot 2H_2O$ [bpe = bis(4-pyridyl)ethane] (**3**), $[Co_2(bpe)_3(SO_4)_2(MeOH)_2]\cdot x$Solv (**4**) and $[Ni_6(bpe)_{10}(H_2O)_{16}](SO_4)_6\cdot xH_2O$ (**5**). In compounds **1–4** the SO_4^{2-} anions are directly involved in the polymeric frameworks, forming bridges that connect different metal centres. Compound **1** contains one-dimensional ribbons of rings joined by the anions to give a 3D array with the $CdSO_4$-type topology. In compound **2** the Cd^{2+} cations are connected by μ_4–η^4-bridging anions to give 2D layers of linked octahedra and tetrahedra, that are joined by the bpethy ligands into a 3D array. The structure of compound **3** consists of simple Cu(bpe) chains linked by the anions into 2D sheets. Compound **4** is a complex polymer comprised of highly undulated 2D layers of folded quadrilateral meshes; the layers are deeply interdigitated and joined together by the anions, thus resulting in an unique 3D architecture containining 6- and 4-connected cobalt centres. Compound **5** is the more interesting species in that it is an entangled array of three distinct sets of layers. It contains two different types of 4-connected 2D motifs, *i.e.* undulated layers of rectangular meshes and square grid layers, in a ratio of 2 : 1. The three sets are parallel to a common axis but show a relative rotation of *ca.* 120° about it, giving a common axis, giving inclined interweaving in an unprecedented 'parallel/parallel/parallel' fashion, to generate a unique 3D architecture.

Introduction

Coordination networks[1] are of great current interest both for their potential applications as new zeolite-like materials[2] for molecular selection, ion exchange and catalysis, and for their intriguing architectures and topologies. New topological types, unprecedented in inorganic compounds and in minerals, can be observed within coordination polymer frameworks. Particularly intriguing is the finding of frames with novel modes of supramolecular entanglements, that contribute to increasing our knowledge of the self-assembly processes and of the supramolecular self-organization of these species. The influence of the anions is fundamental in these processes, especially when they can be directly involved in coordination to the metal centres. Indeed, doubly charged anions like sulfates are known to often enter the inner coordination sphere of metal complexes. Some remarkable examples of polymeric species containing SO_4^{2-} anions have been reported in recent years, including the complicated polycatenated networks $[Cu_2(bpe)_3(H_2O)_2(SO_4)_2]\cdot 2H_2O$ [bpe = bis(4-pyridyl)ethane],[3] $[Co_5(bpe)_9(H_2O)_8(SO_4)_4](SO_4)\cdot 14H_2O$,[4] and $[Cu_5(bpp)_8(SO_4)_4(EtOH)(H_2O)_5](SO_4)\cdot EtOH\cdot 25.5H_2O$ [bpp = bis(4-pyridyl)-propane],[5] and the self-penetrating 3D frame $[Cu(bpe)_2(SO_4)]\cdot 5H_2O$.[6] We report here on five new polymeric species assembled using three bis(4-pyridyl) spacer ligands and some MSO_4 salts ($M^{2+} = Fe^{2+}, Cd^{2+}, Cu^{2+}, Co^{2+}, Ni^{2+}$), namely $[Fe(bpp)_2(SO_4)]$ [bpp = bis(4-pyridyl)propane] (**1**), $[Cd(bpethy)(SO_4)]$ [bpethy = bis(4-pyridyl)ethyne] (**2**), $[Cu(bpe)(SO_4)(H_2O)]\cdot 2H_2O$ [bpe = bis(4-pyridyl)ethane] (**3**), $[Co_2(bpe)_3(SO_4)_2(MeOH)_2]\cdot x$Solv (**4**) and $[Ni_6(bpe)_{10}(H_2O)_{16}](SO_4)_6\cdot xH_2O$ (**5**). They exhibit interesting structural motifs that will be discussed taking into account also the different role of the anions. Within these species, compound **5** is particularly remarkable, showing, for the first time, the polycatenation of three sets of (structurally different) 2D layers rotated about a common axis.

Experimental

Materials

The bpethy [bis(4-pyridyl)ethyne] ligand was prepared according to literature data.[7] All the other reagents and solvents employed were commercially available high-grade purity materials (Aldrich Chemicals), used as supplied, without further purification. Elemental analyses were carried out at the Microanalytical laboratory of this university.

Synthesis of the polymeric compounds

Compound 1. bpp (30.2 mg, 0.152 mmol) was dissolved in methanol (6 mL) and layered on a methanolic solution (8 mL) of $FeSO_4\cdot 7H_2O$ (22.8 mg, 0.0820 mmol). The mixture was left at room temperature for several days, and then the formation of a small amount of a yellow precipitate was noted. The uncharacterized precipitate was removed by filtration and the solution refluxed for 2 h; slow cooling of the hot solution gave small flat yellow crystals of **1** suitable for the X-ray diffractometric analysis. Due to the low yield it was not possible to carry out other characterizations.

Compound 2. An ethanolic solution (4 mL) of the bpethy ligand (22.8 mg, 0.13 mmol) was layered on a solution of $CdSO_4\cdot 8/3H_2O$ (15.2 mg, 0.059 mmol) dissolved in a 1 : 1 mixture of H_2O/EtOH (8 mL). The formation of a white

 DOI: 10.1039/b304201d

Table 1 Crystal data for all compounds

Compound	**1**	**2**	**3**	**4**	**5**
Formula	$C_{26}H_{28}FeN_4O_4S$	$C_{12}H_8CdN_2O_4S$	$C_{12}H_{18}CuN_2O_7S$	$C_{38}H_{44}Co_2N_6O_{10}S_2$	$C_{120}H_{152}N_{20}Ni_6O_{40}S_6$
M	548.43	388.66	397.88	926.77	3059.24
Crystal system	Monoclinic	Tetragonal	Triclinic	Monoclinic	Monoclinic
Space group	$C\,2/c$ (15)	$P\text{-}42_1m$ (113)	$P\text{-}1$ (2)	$C2/c$ (15)	$P\,2_1/c$ (14)
a/Å	21.731(4)	6.831(1)	9.399(3)	23.350(11)	21.485(3)
b/Å	10.588(2)	6.831(1)	9.496(3)	19.882(9)	27.235(4)
c/Å	11.685(2)	14.404(2)	10.073(4)	13.644(6)	26.925(4)
α/°	90	90	62.11(2)	90	90
β/°	110.50(3)	90	89.18(2)	106.29(2)	90.24(1)
γ/°	90	90	73.00(2)	90	90
U/Å^3	2518.3(9)	672.06(17)	751.9(5)	6080(5)	15755(4)
Z	4	2	2	4	4
Density/g cm^{-3}	1.447	1.921	1.757	1.013	1.290
μ(Mo-Kα)/mm^{-1}	0.722	1.793	1.630	0.657	0.858
θ range/°	2–26	2–30	3–25	2–23	2–21
Reflections collected	11645	10709	2620	4869	55661
Indep. refls, R(int)	2448, 0.0640	1124, 0.0394	2620, 0.0	2960, 0.0566	16820, 0.0973
Parameters/restrain	165/1	65/0	211/0	264/209	830/1015
Observed [$F > 4\sigma(F)$]	1596	1051	2001	1671	8930
$R1$ [$F > 4\sigma(F)$]	0.0358	0.0208	0.0439	0.0679[a]	0.1123[a]
$wR2$ (all data)	0.0817	0.0483	0.1312	0.1921[a]	0.3173[a]

[a] values after SQUEEZE (see text).

precipitate was immediately noted, and on leaving the mixture in the dark for several days flat crystals of **2** formed on the walls of the vessel. The white material was recovered by filtration, washed with small amounts of ethanol and dried in air (yield: 65%). Elemental analysis calc. for $C_{12}H_8CdN_2O_4S$: C, 37.08; H, 2.07; N, 7.21%. Found: C, 36.98; H, 2.21; N, 7.15%.

Compound 3. An ethanolic solution (2 mL) of bpe (41.3 mg; 0.224 mmol) was added to an aqueous solution (3 mL) of $Cu(SO_4)\cdot 5H_2O$ (55.9 mg; 0.224 mmol) while stirring. A blue precipitate was formed and the reaction mixture was left to react for about 40 min. The precipitate was filtered through a Buchner funnel, washed with small portions of ethanol and dried in air (yield: 68%). Elemental analysis calc. for $C_{12}H_{18}CuN_2O_7S$: C, 36.22; H, 4.56; N, 7.04%. Found: C, 36.90; H, 4.40; N, 7.25%. Single elongated blue crystals of compound **3**, suitable for the diffractometric analysis, were grown as a minor component together with major amounts of crystals of the already reported species $[Cu(bpe)_2(SO_4)]\cdot 5H_2O$,[6] by slow diffusion of an ethanolic solution of the ligand in an aqueous solution of the metal in a 1 : 2 metal-to-ligand ratio.

Compound 4. An ethanolic solution (30 mM) of the bpe ligand (2 mL, 0.06 mmol) was layered on 2 mL of a methanolic solution of $CoSO_4\cdot 7H_2O$ (8.43 mg; 0.030 mmol). After an initial precipitation of a powdered uncharacterized material, the formation of crystals of compound **4** was noted. On removing these crystals from the mother liquor, amorphous powder immediately formed, preventing further analyses. The high instability of the product required performing the crystallographic data collection after sealing a crystal in a capillary tube in the presence of the mother liquor.

Compound 5. An ethanolic solution (5 mL) of bpe (27.5 mg, 0.149 mmol) was layered on an aqueous solution (5mL) of $NiSO_4\cdot 7H_2O$ (21.4 mg, 0.0762 mmol) after 2 mL of pure ethanol. The mixture was left at 4 °C for some days and then it was allowed to reach the room temperature. The slow evaporation of the solvent almost to dryness left pale green crystals of **5**, which were collected by filtration, washed with small portions of ethanol and dried in the air (yield: 26 mg). The elemental analyses performed on different samples of compound **5** gave variable results, evidencing that the amounts of residual guest solvents were not constant.

Crystallography

Crystal data for all the compounds examined are reported in Table 1. Selected bond distances and angles are given in Tables 2–6. The data collections were performed by the ω-scan method, using Mo-Kα radiation (λ = 0.71073 Å), at room temperature on a SMART-CCD Bruker diffractometer for all the compounds but for **3**, that was collected on an Enraf-Nonius CAD4 instrument. Empirical absorption corrections (SADABS)[8] were applied to the data collected on the SMART-CCD, while ψ-scan method was used for **3**. The structures were solved by direct methods (SIR97)[9] and refined by full-matrix least-squares on F^2 (SHELX-97)[10] with WINGX interface.[11] Anisotropic thermal parameters were assigned to all the non-hydrogen atoms for **1–4**. All hydrogen atoms were placed in geometrically calculated positions and thereafter refined using a riding model with $U_{iso}(H) = 1.2U_{eq}(C)$. The handedness of the crystal of **2** was determined by testing the two enantiomeric models, with a final absolute structure parameter refined to 0.27(5). All the diagrams were performed using the SCHAKAL99 program.[12]

Table 2 Selected bond lengths (Å) and angles (°) for **1**

Fe-O(1)	2.0239(16)
Fe-N(1)	2.248(2)
Fe-N(2)#2	2.252(2)
O(1)#1-Fe-N(1)	90.57(8)
O(1)-Fe-N(1)	89.43(8)
O(1)#1-Fe-N(2)#2	90.74(8)
O(1)-Fe-N(2)#2	89.26(8)
N(1)-Fe-N(2)#2	86.11(7)
N(1)#1-Fe-N(2)#2	93.89(7)

Symmetry transformations used to generate equivalent atoms: #1 $-x+1, -y, -z+1$; #2 $-x+1/2, -y+1/2, -z+1$

Table 3 Selected bond lengths (Å) and angles (°) for **2**

Cd-O	2.2789(14)
Cd-N(10)#4	2.339(3)
Cd-N(1)	2.407(3)
O#1-Cd-O	92.0(2)
O#2-Cd-O	160.88(8)
O#3-Cd-O	84.8(2)
O-Cd-N(10)#4	99.56(4)
O-Cd-N(1)	80.44(4)

Symmetry transformations used to generate equivalent atoms: #1 $-y-1/2, -x-1/2, z$; #2 $-x-1, -y, z$; #3 $y-1/2, x+1/2, z$; #4 $x, y, z-1$

Table 4 Selected bond lengths (Å) and angles (°) for **3**

Cu(1)-O(1S)	2.001(3)
Cu(1)-N(1)	2.010(4)
Cu(1)-O(2)#2	2.381(3)
Cu(2)-O(1)	1.946(3)
Cu(2)-N(2)	2.009(4)
O(1S)#1-Cu(1)-N(1)	89.74(15)
O(1S)-Cu(1)-N(1)	90.26(15)
O(1S)#1-Cu(1)-O(2)#2	90.59(14)
O(1S)-Cu(1)-O(2)#2	89.41(14)
N(1)-Cu(1)-O(2)#2	88.22(14)
N(1)#1-Cu(1)-O(2)#2	91.78(14)
O(1)#3-Cu(2)-N(2)	90.51(16)
O(1)-Cu(2)-N(2)	89.49(16)

Symmetry transformations used to generate equivalent atoms: #1 $-x+1$, $-y$, $-z+1$; #2 $x+1$, y, z; #3 $-x$, $-y$, $-z+1$

Table 5 Selected bond lengths (Å) and angles (°) for **4**

Co(1)-O(2)	2.068(4)
Co(1)-N(1)	2.168(6)
Co(1)-N(3)	2.175(8)
Co(2)-O(1)#2	2.083(5)
Co(2)-O(1S)	2.101(6)
Co(2)-N(2)	2.148(7)
O(2)-Co(1)-N(1)	91.0(2)
O(2)#1-Co(1)-N(1)	89.0(2)
O(2)-Co(1)-N(3)#1	90.4(2)
N(1)-Co(1)-N(3)#1	87.1(3)
O(2)-Co(1)-N(3)	89.6(2)
N(1)-Co(1)-N(3)	92.9(3)
O(1)#2-Co(2)-O(1)#3	176.6(3)
O(1)#2-Co(2)-O(1S)	90.0(2)
O(1)#3-Co(2)-O(1S)	87.7(2)
O(1S)#4-Co(2)-O(1S)	93.9(4)
O(1S)-Co(2)-N(2)#4	175.8(2)
O(1)#2-Co(2)-N(2)	90.0(2)
O(1)#3-Co(2)-N(2)	92.4(2)
O(1S)-Co(2)-N(2)	89.6(3)
N(2)#4-Co(2)-N(2)	87.1(4)

Symmetry transformations used to generate equivalent atoms: #1 $-x+1/2$, $-y+1/2$, $-z+1$; #2 $x-1/2$, $y+1/2$, z; #3 $-x+1/2$, $y+1/2$, $-z+3/2$; #4 $-x$, y, $-z+3/2$

The crystal of **4** loses solvent quickly and therefore it was sealed into a capillary tube for the collection; notwithstanding the crystal decomposes during the data collection and significant data were measured for a partial sphere (70%) up to $\theta = 23°$. The structure of compound **5** was recognized to be twinned by merohedry and a suitable set of BASF/TWIN parameters was used in the refinement, according to the procedure described in SHELX for the monoclinic system, with β approxymately 90°, that may emulate the orthorhombic system: twin law [1 0 0, 0 −1 0, 0 0 −1], final refined factor 0.198(2). Moreover **5** was refined with all the light atoms isotropic because of a weak intensity set of data and in order to keep a reasonable parameters to observations ratio. Both **4** and **5** present large solvent-accessible volumes, that were assessed using the PLATON software,[13] and the contribution of the disordered solvent (located in the voids) to the diffraction pattern was subtracted from the observed data by the "Squeeze" method, as implemented in PLATON.[14] The final R1 values [$I > 2\sigma(I)$] before SQUEEZE were 0.116 and 0.173 for **4** and **5**, respectively.

CCDC reference numbers 208665–208669. See http://www.rsc.org/suppdata/ce/b3/b304201d/ for crystallographic data in CIF or other electronic format.

Results and discussion

All the polymeric products **1–5** have been obtained as crystalline materials, by slow diffusion methods, and characterized by single crystal X-ray analyses. Some of them, as **5** and, especially, **4** are rather instable in air.

Compound **3** was previously obtained as a minor crystalline product in the crystallization from H_2O/ethanol solutions of the self-penetrating 3D species $[Cu(bpe)_2(SO_4)]\cdot 5H_2O$, as we have already reported elsewhere.[6] The occurrence of mixtures of products is rather common in coordination polymer chemistry since subtle factors, difficult to rationalize, can

Table 6 Selected bond lengths (Å) and angles (°) for **5**

Ni(1)-O(11L)	2.089(12)	N(6)#2-Ni(2)-O(22L)	88.6(5)
Ni(1)-O(12L)	2.094(10)	N(4)-Ni(2)-O(22L)	88.1(5)
Ni(1)-N(1)	2.108(13)	O(24L)-Ni(2)-O(22L)	93.4(4)
Ni(1)-N(3)	2.145(13)	O(21L)-Ni(2)-O(22L)	88.9(4)
Ni(1)-N(5)	2.147(13)	N(10)-Ni(3)-O(31L)	87.6(5)
Ni(1)-N(2)#1	2.154(13)	N(10)-Ni(3)-N(14)	90.8(5)
Ni(2)-O(23L)	2.074(12)	O(31L)-Ni(3)-N(14)	86.9(5)
Ni(2)-N(6)#2	2.079(14)	N(10)-Ni(3)-N(7)	179.0(5)
Ni(2)-N(4)	2.105(14)	O(31L)-Ni(3)-N(7)	92.5(5)
Ni(2)-O(24L)	2.116(12)	N(14)-Ni(3)-N(7)	88.2(5)
Ni(2)-O(21L)	2.116(12)	N(10)-Ni(3)-N(12)	91.1(5)
Ni(2)-O(22L)	2.125(10)	O(31L)-Ni(3)-N(12)	89.2(5)
Ni(3)-N(10)	2.071(13)	N(14)-Ni(3)-N(12)	175.6(5)
Ni(3)-O(31L)	2.099(12)	N(7)-Ni(3)-N(12)	89.8(5)
Ni(3)-N(14)	2.101(13)	N(10)-Ni(3)-O(32L)	89.8(5)
Ni(3)-N(7)	2.116(13)	O(31L)-Ni(3)-O(32L)	177.0(5)
Ni(3)-N(12)	2.123(13)	N(14)-Ni(3)-O(32L)	91.8(5)
Ni(3)-O(32L)	2.141(11)	N(7)-Ni(3)-O(32L)	90.2(5)
Ni(4)-O(41L)	2.047(11)	N(12)-Ni(3)-O(32L)	92.2(5)
Ni(4)-O(42L)	2.069(11)	O(41L)-Ni(4)-O(42L)	176.1(4)
Ni(4)-N(9)#3	2.104(12)	O(41L)-Ni(4)-N(9)#3	91.9(5)
Ni(4)-N(8)#4	2.108(11)	O(42L)-Ni(4)-N(9)#3	92.0(5)
Ni(4)-N(11)	2.156(13)	O(41L)-Ni(4)-N(8)#4	88.0(5)
Ni(4)-N(13)#5	2.195(13)	O(42L)-Ni(4)-N(8)#4	88.1(5)
Ni(5)-N(16)	2.070(14)	N(9)#3-Ni(4)-N(8)#4	179.2(5)
Ni(5)-N(18)	2.077(14)	O(41L)-Ni(4)-N(11)	90.4(4)
Ni(5)-O(52L)	2.114(11)	O(42L)-Ni(4)-N(11)	89.6(5)
Ni(5)-O(51L)	2.121(10)	N(9)#3-Ni(4)-N(11)	90.1(5)
Ni(5)-N(20)	2.127(12)	N(8)#4-Ni(4)-N(11)	89.1(5)
Ni(5)-N(19)	2.134(12)	O(41L)-Ni(4)-N(13)#5	87.7(5)
Ni(6)-O(62L)	2.060(13)	O(42L)-Ni(4)-N(13)#5	92.4(5)
Ni(6)-O(63L)	2.063(11)	N(9)#3-Ni(4)-N(13)#5	89.0(5)
Ni(6)-O(61L)	2.087(11)	N(8)#4-Ni(4)-N(13)#5	91.8(5)
Ni(6)-N(15)	2.096(13)	N(11)-Ni(4)-N(13)#5	177.9(5)
Ni(6)-O(64L)	2.115(12)	N(16)-Ni(5)-N(18)	175.9(6)
Ni(6)-N(17)	2.136(14)	N(16)-Ni(5)-O(52L)	91.9(5)
		N(18)-Ni(5)-O(52L)	91.9(5)
O(11L)-Ni(1)-O(12L)	178.3(4)	N(16)-Ni(5)-O(51L)	89.1(5)
O(11L)-Ni(1)-N(1)	89.7(5)	N(18)-Ni(5)-O(51L)	87.0(5)
O(12L)-Ni(1)-N(1)	92.0(5)	O(52L)-Ni(5)-O(51L)	178.1(4)
O(11L)-Ni(1)-N(3)	89.5(5)	N(16)-Ni(5)-N(20)	89.5(5)
O(12L)-Ni(1)-N(3)	90.6(4)	N(18)-Ni(5)-N(20)	92.1(5)
N(1)-Ni(1)-N(3)	93.3(5)	O(52L)-Ni(5)-N(20)	86.5(4)
O(11L)-Ni(1)-N(5)	89.9(5)	O(51L)-Ni(5)-N(20)	91.9(4)
O(12L)-Ni(1)-N(5)	90.0(5)	N(16)-Ni(5)-N(19)	89.5(5)
N(1)-Ni(1)-N(5)	89.2(5)	N(18)-Ni(5)-N(19)	89.1(5)
N(3)-Ni(1)-N(5)	177.5(5)	O(52L)-Ni(5)-N(19)	91.4(4)
O(11L)-Ni(1)-N(2)#1	88.8(5)	O(51L)-Ni(5)-N(19)	90.2(4)
O(12L)-Ni(1)-N(2)#1	89.6(4)	N(20)-Ni(5)-N(19)	177.7(5)
N(1)-Ni(1)-N(2)#1	176.9(5)	O(62L)-Ni(6)-O(63L)	86.9(5)
N(3)-Ni(1)-N(2)#1	89.4(5)	O(62L)-Ni(6)-O(61L)	94.0(5)
N(5)-Ni(1)-N(2)#1	88.2(5)	O(63L)-Ni(6)-O(61L)	178.6(4)
O(23L)-Ni(2)-N(6)#2	91.3(5)	O(62L)-Ni(6)-N(15)	90.3(5)
O(23L)-Ni(2)-N(4)	92.1(5)	O(63L)-Ni(6)-N(15)	89.8(5)
N(6)#2-Ni(2)-N(4)	176.1(5)	O(61L)-Ni(6)-N(15)	89.0(5)
O(23L)-Ni(2)-O(24L)	88.5(5)	O(62L)-Ni(6)-O(64L)	176.3(5)
N(6)#2-Ni(2)-O(24L)	87.2(5)	O(63L)-Ni(6)-O(64L)	90.1(4)
N(4)-Ni(2)-O(24L)	90.9(5)	O(61L)-Ni(6)-O(64L)	89.1(4)
O(23L)-Ni(2)-O(21L)	89.2(5)	N(15)-Ni(6)-O(64L)	91.8(5)
N(6)#2-Ni(2)-O(21L)	93.4(5)	O(62L)-Ni(6)-N(17)	87.5(5)
N(4)-Ni(2)-O(21L)	88.6(5)	O(63L)-Ni(6)-N(17)	93.4(5)
O(24L)-Ni(2)-O(21L)	177.6(5)	O(61L)-Ni(6)-N(17)	87.9(5)
O(23L)-Ni(2)-O(22L)	178.1(5)	N(15)-Ni(6)-N(17)	176.0(5)
		O(64L)-Ni(6)-N(17)	90.7(5)

Symmetry transformations used to generate equivalent atoms: #1 $-x$, $y+1/2$, $-z+1/2$; #2 $x+1$, $-y+5/2$, $z+1/2$; #3 x, $-y-1/2$, $z-1/2$; #4 x, $-y-1/2$, $z+1/2$; #5 x, $y-1$, z

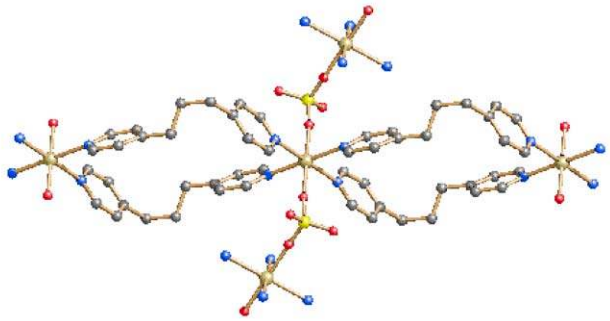

Fig. 1 A view of a ribbon of rings in **1**. The octahedral coordination at the Fe^{2+} centres and the conformation of the ligands are illustrated.

drive the self-assembly processes. It is interesting to note that Zubieta and coworkers, using the same reagents, have previously obtained by hydrothermal syntheses two different species, $[Cu_2(bpe)_3(H_2O)_2(SO_4)_2]\cdot 2H_2O$ and $[Cu(bpe)(SO_4)(H_2O)]$.[3] The latter is a *pseudo*-polymorph of **3**, but their structures are completely different (see below).

Description of the structures

The structure of compound **1** consists of one-dimensional polymeric ribbons of rings in which two bpp ligands, in the *gauche-trans* conformation, act as bridges joining adjacent Fe^{2+} ions, with a Fe···Fe separation of 12.09 Å (Fig. 1).

Each metal is bound to four equatorial pyridyl groups [Fe–N 2.248(2), 2.252(2) Å] and to two axial oxygen atoms of two sulfate anions [Fe–O 2.024(2) Å] in an octahedral environment. Such ribbons represent a rather common structural motif in coordination polymer chemistry, and were previously observed in species containing various bidentate flexible ligands. Examples with bpp ligands are $[M(bpp)_2(H_2O)_2](ClO_4)_2\cdot bpp\cdot H_2O$ (M = Ni, Co)[15] and $[Ni(bpp)_2(H_2O)_2](NO_3)_2\cdot bpp\cdot H_2O$.[16] The peculiarity of **1** is that the 1D ribbons span two different directions of propagation, *i.e.* [1 1 0] and [1 −1 0], on alternating planes stacking perpendicular to the crystallographic ***c***-axis. The μ–η^2-SO_4^{2-} anions bridge the two sets of ribbons (Fe···Fe separation of 5.84 Å) thus generating an overall 3D single network (as shown in Fig. 2). The topology of this 4-connected net is of the $CdSO_4$ type [short and long Schläfli symbols ($6^5\cdot 8$) and ($6\cdot 6\cdot 6\cdot 6\cdot 6_2\cdot\infty$)], and is schematically illustrated in Fig. 3. The sphere packing (Fig. 2c) shows that no residual space is left.

Compound **2** exhibits a structure that can be related to some 'organic–inorganic' polymeric species described by Zubieta *et al.*,[1d,17] containing molybdate instead of sulfate counterions, as [Cu(bpe)(MoO_4)] (MOXI-1).[18] In **2** the [Cd(SO_4)] sublattice consists of layers in which the SO_4^{2-} anions are μ_4–η^4-bridging on four metal centres. The Cd^{2+} ions interact with four equatorial O(SO_4^{2-}) atoms [Cd-O 2.279(1) Å] and two axial

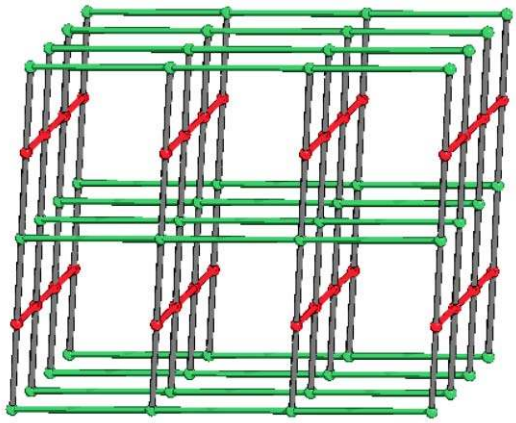

Fig. 3 Schematic view of the 4-connected network topology ($CdSO_4$-type) in **1**. The green and red lines represent the two sets of polymeric chains, while the gray lines represent the bridging sulfate.

N(pyridyl) atoms [Cd–N 2.339(3), 2.407(3) Å] in a distorted octahedral environment. The metal ion is well displaced out of the equatorial O_4 plane [O–Cd–N angles by one side 99.56(4)° *vs.* 80.44(4)° by the opposite side].

These 4-connected layers (Fig. 4) are comprised of alternating octahedral and tetrahedral units (in the ratio 1 : 1), with Cd···Cd shortest contacts of 4.93 Å.

Interestingly, the layers differ from those observed in the related species [Cu(bpe)(MoO_4)], in which the MoO_4^{2-} tetrahedra are μ_3–η^3-bridging and the Cu^{2+} centers are in a trigonal bipyramidal environment, comprising two axially bonded pyridyl groups. The bpethy ligands connect these layers (stacking sequence *AAA*) into a 3D array (Fig. 5, left), with an interlayer spacing corresponding to the ***c***-axis (14.4 Å). The packing (Fig. 5, middle and right) leaves 10% of voids in channels of square section (*ca.* 2.0 × 2.5 Å) running along the [1 1 0] or [1 −1 0] directions (Fig. 5, right). In [Cu(bpe)(MoO_4)] the interlayer separation is smaller, 11.0 Å. Similar inorganic layers separated in a controlled fashion by organic spacers can be, in principle, obtained by using $M^{II}SO_4$ salts and linear bidentate spacers of different length in the ratio 1 : 1. Within this family we have also isolated a species of composition [Cd(pyrazine)(SO_4)], in which the layers exhibit a spacing of 7.42 Å.[19]

The structure of $[Cu(bpe)(SO_4)(H_2O)]\cdot 2H_2O$ (**3**), containing a metal-to-ligand ratio of 1 : 1, is much less complex than that of the other product obtained from the same reaction mixture, *i.e.* the previously reported self-penetrating 3D species $[Cu(bpe)_2(SO_4)]\cdot 5H_2O$ [exhibiting a binodal ($6^4\cdot 8^2$)($6\cdot 8^5$) topology].[6] It simply consists of 1D zig-zag chains –bpe-Cu-bpe-Cu–, with the ligands in the *gauche* conformation, all running in the [2 −1 0] direction and showing a Cu···Cu separation of 9.21 Å (see Fig. 6).

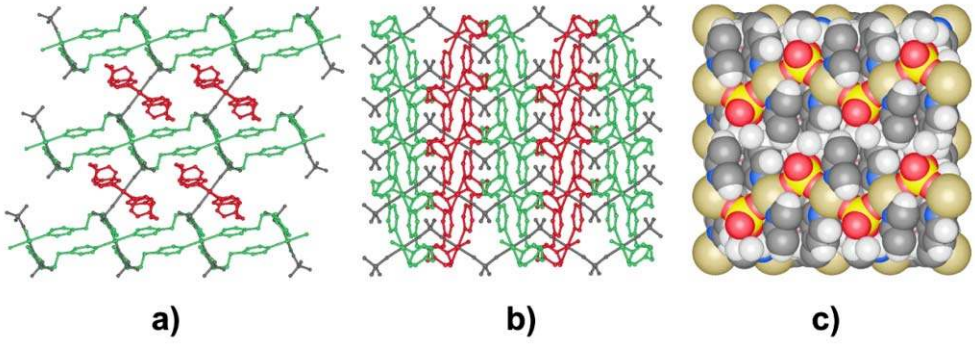

Fig. 2 Two views of the 3D network in **1** (a) and (b). The two sets of differently oriented ribbons are shown (in green and red), as well as the bridging sulfates (in gray). The sphere packing is illustrated in (c). Click here to access a 3D representation.

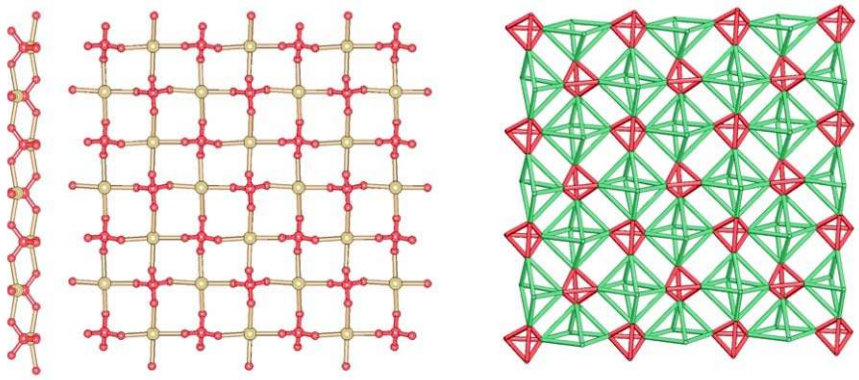

Fig. 4 The [Cd(SO_4)] sublattice in **2**. Side and front views of one layer (left and middle) and the representation with the vertex-linked alternating octahedra and tetrahedra (right).

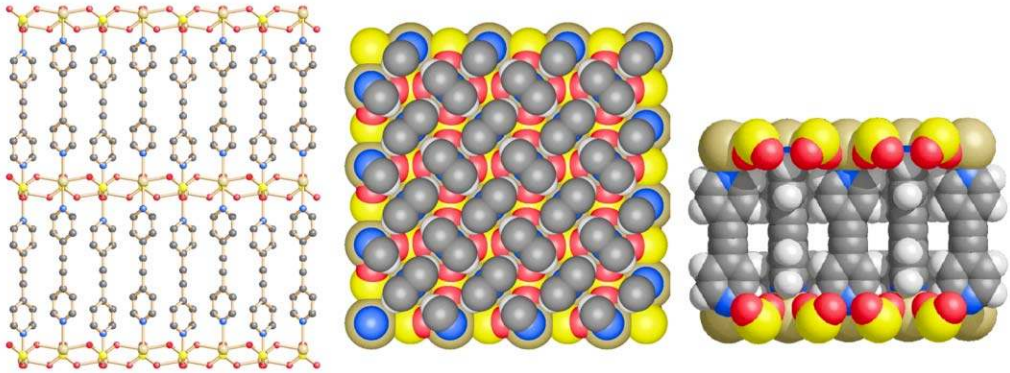

Fig. 5 A view of the network in **2**, illustrating the interlayer connections (left) and two views of the sphere packing down the ***c***-axis (middle) and along the [1 1 0] direction, showing the channels (right). The herringbone disposition of the ligand planes of adjacent rows is evident in the middle and right views. Click here to access a 3D representation.

The chains are joined by μ–η^2-bridging sulfates (Cu···Cu separation of 4.75 Å) to give 2D (4,4)-layers of rectangular meshes (Fig. 7). Along the chains there are two alternating independent Cu^{2+} atoms, both lying on inversion centers, that display different coordination spheres: Cu1 is Jahn–Teller elongated octahedral [Cu–N 2.010(4), Cu–O(H_2O) 2.001(3), Cu–O(SO_4^{2-}) 2.381(3) Å), Cu2 is square planar [Cu–N 2.009(4), Cu–O(SO_4^{2-}) 1.946(3) Å]. The resulting 2D layers stack along the direction of the ***c***-axis, with a separation of 1/2***c***. (5.04 Å). The coordinated and solvated water molecules are connected by intralayer hydrogen bonding (O···O range 2.72–2.86 Å), resulting in a packing with no voids left. It is worth to compare this structure with that of its *pseudo*-polymorph [Cu(bpe)(SO_4)(H_2O)], not containing solvated water molecules.[3] Also this species is based on –bpe-Cu-bpe-Cu– chains joined by double bridging SO_4^{2-} anions. However, the chains are linear because the bpe ligands adopt *trans* conformation (Cu···Cu separation of 13.5 Å) and span two different directions (rotated by *ca.* 82°) on alternate levels, as observed for the ribbons in compound **1**, thus generating a 3D array of the $CdSO_4$ topological type. The network is 2-fold interpenetrated and this can explain the absence of solvated molecules.

The structure of [Co_2(bpe)$_3$(SO_4)$_2$($MeOH$)$_2$]·*x*Solv (**4**) is remarkable for many unusual features. It consists of highly undulated 2D (4,4)-layers sustained by coordinative bonds, containing quadrilateral folded meshes (see Fig. 8 and 9). These circuits are comprised of six metal centres, *i.e.* four tetra-connected Co atoms at the corners and two bi-connected Co atoms at the midpoint of the longer edges. The folding of each mesh occurs about an axis passing through the facing pair of bi-connected metals. The Co···Co distances bridged by the bpe ligands are 13.48 and 13.64 Å and the period of the 'waves', running along the [1 0 −1] direction, is 30.17 Å.

These layers stack with an *ABAB* sequence along the [0 1 0] direction and show a deep mutual interdigitation (see Fig. 10).

The SO_4^{2-} anions play the role of μ–η^2-bridges, by joining the bi-connected metal centres of each layer with the four-connected ones on the adjacent interdigitated upper and lower layers. This generates an overall 3D array with six- and four-connected nodes in the ratio 1 : 1 [short Schläfli symbol $(4^2{\cdot}5^4{\cdot}6^4{\cdot}7{\cdot}8^4)(4^2{\cdot}5^4)$], schematically illustrated in Fig. 10. A detailed analysis of the topology reveals that this single

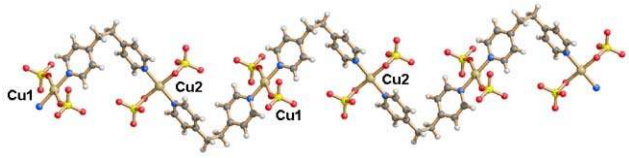

Fig. 6 A zigzag chain in compound **3**. Click here to access a 3D representation.

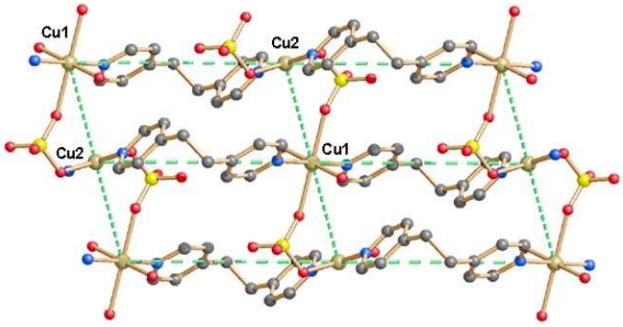

Fig. 7 A view of a (4,4)-layer in **3**, formed by the SO_4^{2-} anions bridging the chains.

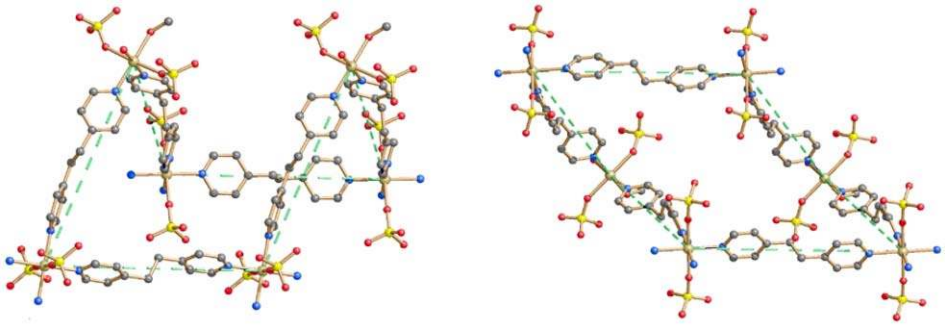

Fig. 8 Two views of a single folded mesh (4-membered ring) within the (4,4)-layers in compound **4**.

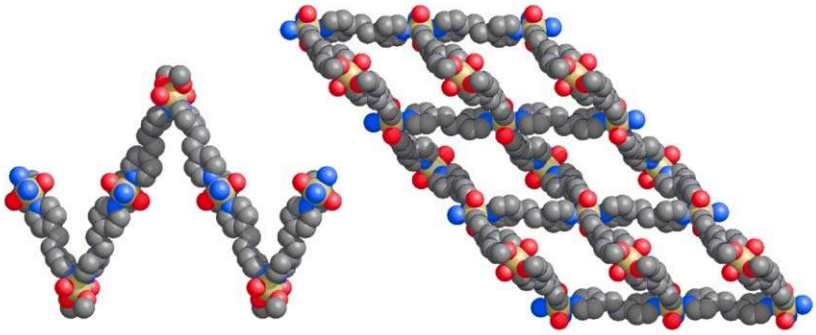

Fig. 9 Side and front views of a (4,4) highly undulated layer in **4**.

network contains 6-membered rings that are intra-catenated (see Fig. 11). It could seem, therefore, a self-penetrating net, but some caution must be exercised about this point. We must refer to the topological classification of nets, represented by their Schläfli symbols; if one of the 'shortest rings'[20] is catenated by other 'shortest rings' of the same net we can speak of a true case of self-penetration. This is a necessary condition to be accomplished, since, otherwise, catenated rings or knots can always be found in any kind of network, provided that sufficiently long circuits are considered. Here the interlaced rings (see Fig. 11) contain four 6-connected and two 4-connected nodes and, since the 'shortest rings' at the 4-connected nodes are only 4-gons and 5-gons, we are not allowed to consider compound **4** a real case of self-penetration.[21]

The coordination geometries of all the cobalt atoms are octahedral: one half of the metals (*i.e.*, those at the corners of the above described quadrilateral meshes, lying on inversion centers) are bonded to four equatorial N(pyridyl) and two axial $O(SO_4^{2-})$ atoms [Co–N 2.168(6), 2.175(8) Å and Co–O 2.068(4) Å], while the coordination sphere of the other cobalt atoms (lying on 2-fold axes) consists of two *cis* N(pyridyl), two *cis* O(MeOH) and two *trans* $O(SO_4^{2-})$ atoms [Co–N 2.148(7) Å, Co–O(MeOH) 2.101(6) Å and Co–$O(SO_4^{2-})$ 2.083(5) Å]. The network contains very large free voids corresponding to *ca.* 42% of the cell volume, mainly located within channels of approximate section 3.5 Å, running along the [1 1 0] direction and filled with disordered solvent molecules (Fig. 12). The open framework structure is responsible for the instability of this species when removed from the solvent.

Compound **5** is a fascinating entangled network with an unprecedented topology. It consists of three distinct sets of 2D (4,4)-layers that span three different spatial orientations and give mutual interweaving. This results in an overall 3D polycatenated architecture, illustrated in Fig. 13. The layers are of two different types, with rectangular (A) and square meshes (B), in the ratio 2 : 1. There are two distinct sets of parallel undulated layers of A

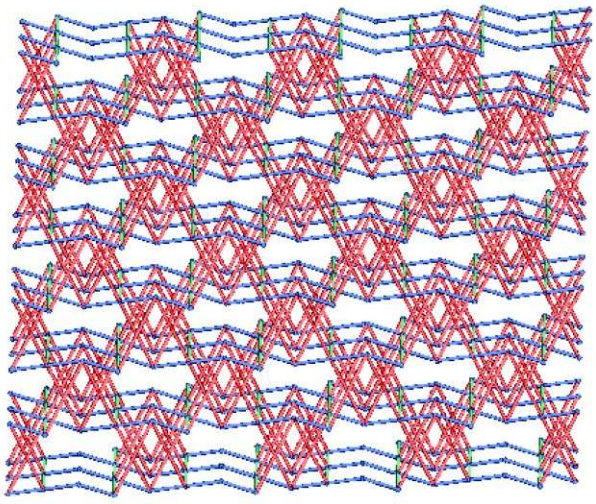

Fig. 10 Schematic illustration of the interdigitation of the undulated layers in **4**. The edges of the 4-membered rings in the layers are in green and red, while the blue contacts represent the sulfate bridges that generate the overall 3D net.

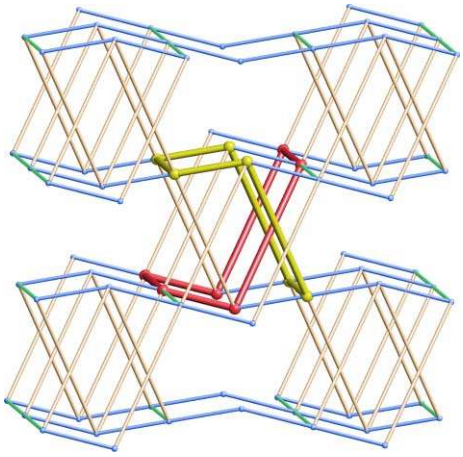

Fig. 11 A portion of the schematized 3D net in **4** showing two catenated 6-membered rings.

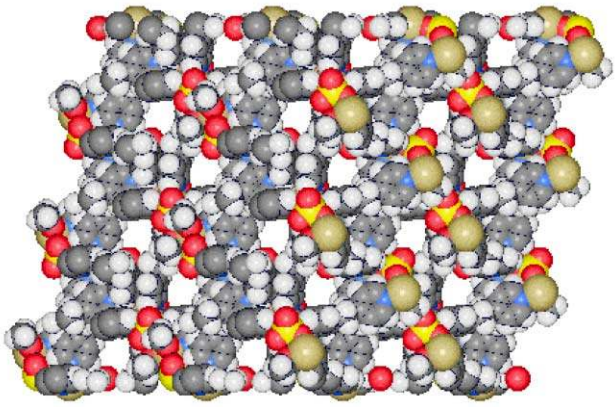

Fig. 12 A view of the sphere packing down [1 1 0] in **4**, showing the main channels.

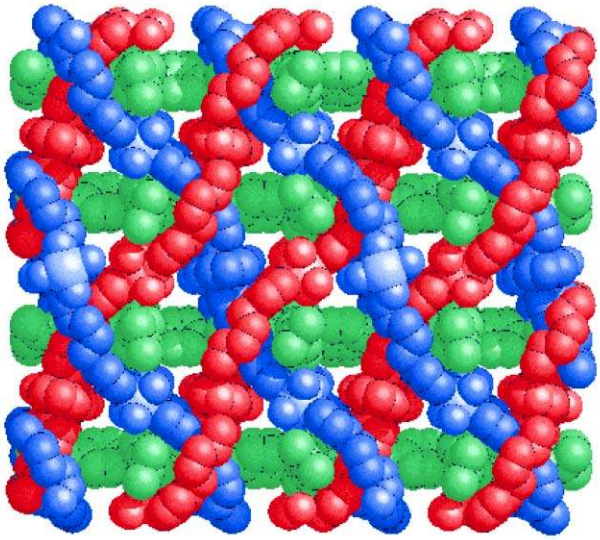

Fig. 13 The polycatenated 3D array in compound **5**, viewed down the *b*-axis. Different colours have been employed for the three distinct sets of layers.

type (in red and blue) that stack along the [1 0 −1] and [1 0 1] directions, respectively, and cross between themselves giving inclined interpenetration. The square meshed layers B (in green) stack along the [1 0 0] direction, thus catenating the other two sets. The three sets are parallel to the ***b*** crystallographic axis and display a relative rotation about this axis of *ca.* 120°.

The A and B layers are shown in Fig. 14. The rectangular windows of the A layers contain six metal centers, four at the corners and two at the midpoint of the longer edges. The dimensions of the windows are 13.6 × 26.1 Å. The stacking sequence of these layers is *ABAB*, with interlayer separation of 11.5 Å. All the Ni metal atoms show an octahedral coordination: those at the corners (Ni1, Ni5) are connected to four equatorial pyridyl groups (Ni–N range 2.07–2.15 Å) and two axial water molecules (Ni–O range 2.09–2.12 Å) while the other ones (Ni2, Ni6), acting simply as spacers, are *trans*-coordinated by two pyridyl groups (Ni–N range 2.08–2.14 Å) and bear four equatorial water molecules (Ni–O range 2.06–2.12 Å).

The B type layers are comprised of almost regular squares of dimensions 13.5 × 13.7 Å, and exhibit a stacking sequence *ABAB*, with an interlayer distance of 10.5 Å. The metal atoms (Ni3, Ni4) display an octahedral coordination geometry, with four equatorial pyridyl groups (Ni–N 2.07–2.19 Å) and two axial H_2O molecules (Ni–O 2.05–2.14 Å).

The most interesting feature of this structure is the unprecedented type of intertwining (schematically shown in Fig. 15). The peculiarities consist in the presence of: (i) structurally different 2D motifs; (ii) three distinct sets of polycatenated planes; and (iii) the particular mode of catenation.

This species belongs to the family of 3D networks derived by inclined interpenetration of 2D layers. There are numerous examples of this class of polycatenated frameworks,[22] the majority of which consist of two identical sets of parallel layers, of (6,3) or (4,4) topology, spanning two different stacking directions. Different modes of interpenetration of the two sets have been considered by Batten and Robson[22a] and by Zaworotko.[1k] Only in few cases, major variations of the above theme were observed. For instance, we have previously reported the unique example within coordination frameworks of the inclined interpenetration involving two sets of 2D layers of different topology, namely $[Ni(azpy)_2(NO_3)_2]_2[Ni_2(azpy)_3(NO_3)_4]\cdot 4CH_2Cl_2$ [azpy = *trans*-4,4′-azobis(pyridine)], containing both (6,3)- and (4,4)-layers.[23]

Another major variation is represented by the presence of more than two distinct sets of layers. No real case was known in 1998 when Batten and Robson had suggested the possibility of finding three different mutually perpendicular stacks;[22a] since then three examples have been reported, to our knowledge, all exhibiting peculiar features, though none exactly with that hypothetical interpenetration mode. The first species to be reported was a network sustained *via* hydrogen-bond bridges in $[Pt(HL)_2L_2]\cdot 2H_2O$ (HL = isonicotinic acid),[24] containing three sets of (4,4) sheets stacking in three 'perpendicular' directions, *i.e.* [1 1 0], [−1 1 0] and [0 0 1] (see Scheme 1, left). Using the terminology for the inclined interpenetration of two stacks of (4,4) layers,[1k] we observe that the interpenetration mode within each pair of sets is of the diagonal–diagonal type (thus, overall diagonal/diagonal/diagonal), and that each square window in one of the sets is catenated by three other layers, while each square window in the other two sets is catenated by five different layers [we can define a sort of 'density of catenation' that can be represented, in this case, by (3/5/5)].[25]

The second example, $[Fe(bpb)_2(NCS)_2]\cdot 0.5MeOH$ [bpb = 1,4-bis(4-pyridyl)butadiyne],[26] is a 3D network entirely based

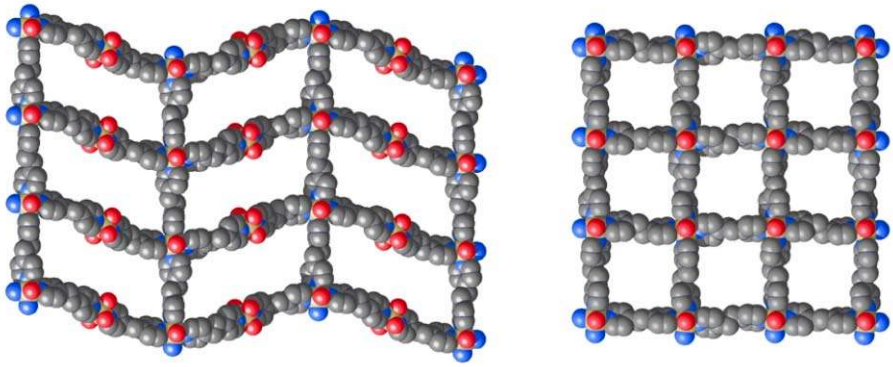

Fig. 14 The two different types of (4,4) layers in **5**: type A are undulating, with rectangular meshes, while type B are more flat, with square meshes.

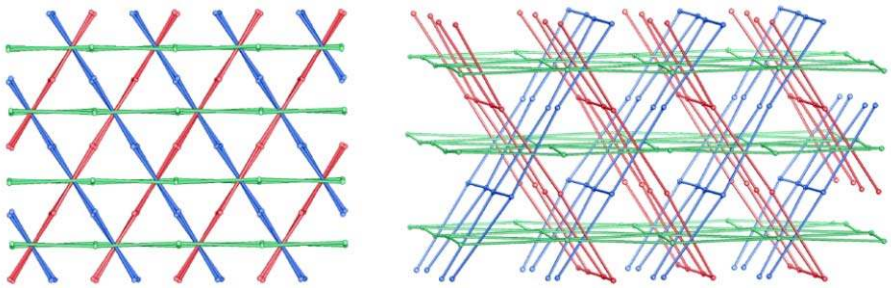

Fig. 15 Two different schematic views of the 3D architecture in **5**.

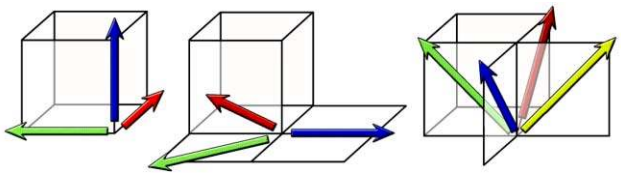

Scheme 1 The stacking directions of the independent sets of layers in the known species containing more than two sets: three almost perpendicular directions in $[Pt(HL)_2L_2]\cdot 2H_2O$ and $[Fe(bpb)_2(NCS)_2]\cdot 0.5MeOH$ (left), three coplanar directions in **5** (middle) and four directions related by the tetragonal axis in $[Co_2(azpy)_3(NO_3)_4]\cdot Me_2CO\cdot 3H_2O$ (right).

on coordinative bonds, similar to the previous one in that it contains three sets of (4,4) layers stacking in three 'perpendicular' directions (Scheme 1, left), *i.e.* [1 1 0], [−1 1 0] and [0 0 1]. Again, the interpenetration mode is diagonal/diagonal/diagonal, with the same 'density of catenation'.

The third example is a quite noteworthy coordination network, $[Co_2(azpy)_3(NO_3)_4]\cdot Me_2CO\cdot 3H_2O$ (azpy = 4,4′-azopyridine),[27] whose entanglement was rather overviewed by the authors. It contains four different sets of (6,3) sheets (brick-wall pattern) that stack along four directions (see Scheme 1, right), *i.e.* [1 0 4], [−1 0 4], [0 1 4], [0 −1 4], related by the four-fold tetragonal axis. The 'density of catenation' is (3/3/3/3).

The interpenetration observed in compound **5** is novel in that the three stacks occur along three coplanar directions (Scheme 1, middle), [1 0 −1], [1 0 1] and [1 0 0], lying in a plane perpendicular to the *b* crystallographic axis. The interpenetration mode (see Fig. 16) can be described as parallel/parallel/parallel. Each rectangular mesh of the A layers is catenated by two inclined layers of the same type A (Fig. 16a) and by two

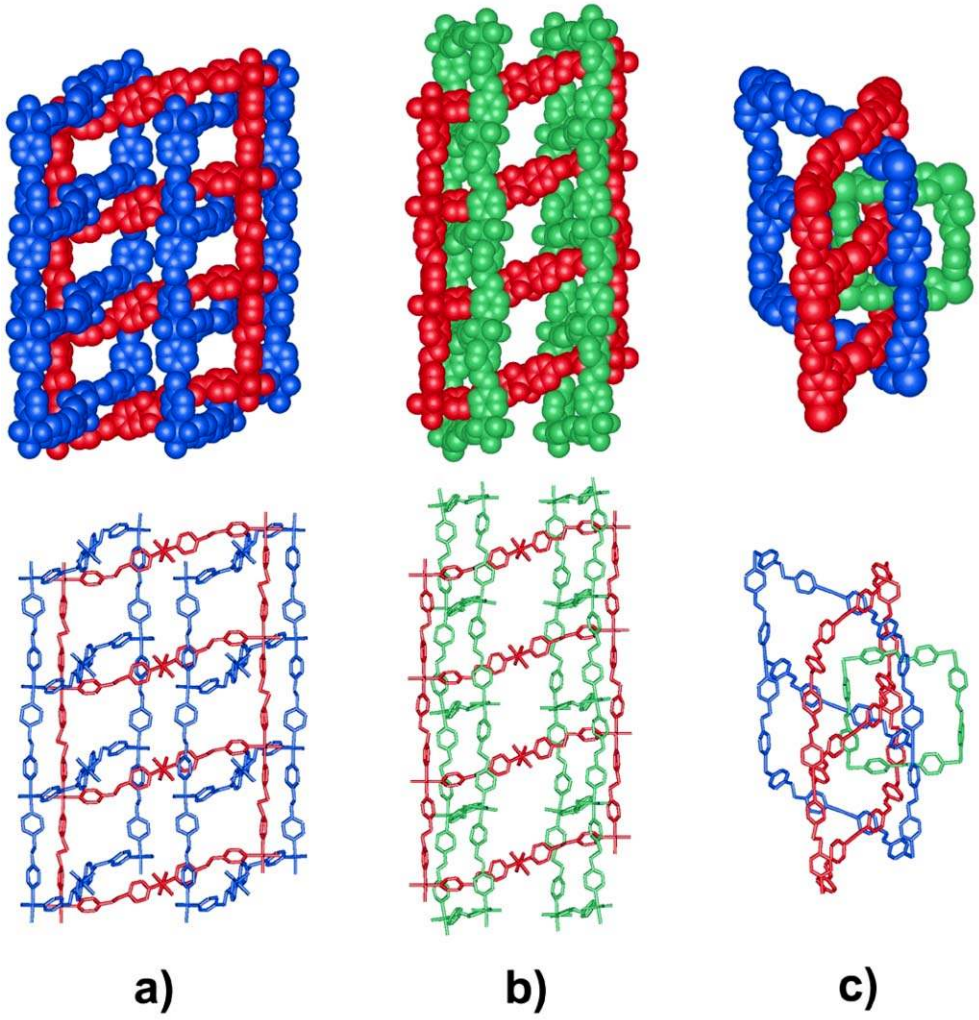

Fig. 16 The polycatenation within the different sets of layers in **5**: (a) type A windows catenated by inclined layers of the same type (A *plus* A); (b) the same A windows catenated also by B type layers (A *plus* B); (c) a B type square catenated by two A layers. Click here to access a 3D representation.

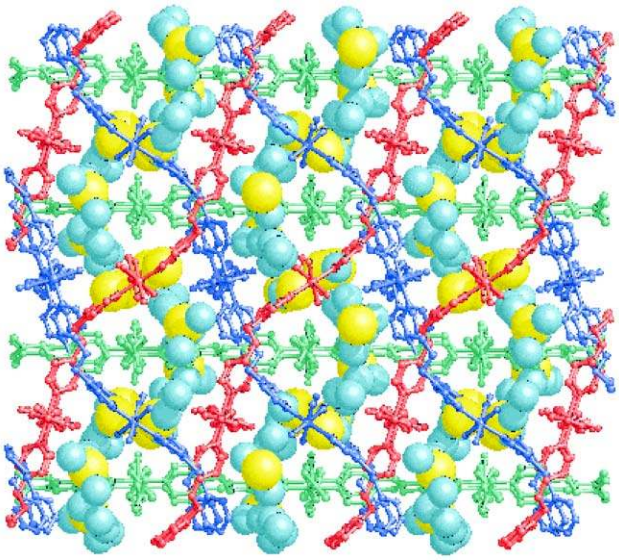

Fig. 17 The snaky channels in the network of **5**, containing the sulfate anions and the solvated water molecules.

layers of type B (Fig. 16b), while a square mesh of the B layers is catenated by one A layer of each of the two sets (Fig. 16c). The 'density of catenation' is, therefore, equal to (2/4/4).

In spite of the polycatenation described above, the network of **5** contains large free voids (*ca.* 19% of the cell volume) disposed in connected chambers that form snaky channels, illustrated in Fig. 17. These channels enclose the sulfate anions and about 28 solvated water molecules per formula unit. The uncoordinated sulfate anions interact *via* hydrogen bonds with the water molecules coordinated to the metal centres (O···O bridges in the range 2.60–2.82 Å), thus resulting in a complicated 3D unique network. Also, in this case the open network structure is likely responsible for a certain instability of the material that slowly decomposes when removed from the mother liquor and left in the air.

Conclusions

We have described here some novel coordination polymers containing sulfates as counterions. Interesting structural motifs have been characterized, including a fascinating species like **5**, with an unprecedented type of polycatenation, of relevance at the basic structural level. These structures confirm that a dianion like sulfate can play an important role in driving the assembly of the polymeric networks because of its relatively high coordinating ability towards metal centres, that often leads to the formation of bridging interactions. In compound **1**, for instance, the peculiar tridimensional organization of the 1D ribbons is strictly related to the presence of the bridging anions. Strong metal–sulfate interactions give rise to inorganic $[CdSO_4]$ 2D layers in **2** and are also responsible for the formation of a unique 3D array in **4**. Compound **5** is exceptional from this point of view since the sulfates are uncoordinated, though they could have had some templating influence in the preliminary steps of the assembly of this species.

References

1 (*a*) B. F. Hoskins and R. Robson, *J. Am. Chem. Soc.*, 1990, **112**, 1546; (*b*) R. Robson, B. F. Abrahams, S. R. Batten, R. W. Gable, B. F. Hoskins and J. Liu, *Supramolecular Architecture*, ACS Symposium Series 499, ed. T. Bein, Am. Chem. Soc., Washington, DC, 1992; (*c*) C. L. Bowes and G. A. Ozin, *Adv. Mater.*, 1996, **8**, 13; (*d*) P. J. Hagrman, D. Hagrman and J. Zubieta, *Angew. Chem. Int. Ed.*, 1999, **38**, 2639; (*e*) M. Munakata, L. P. Wu and T. Kuroda-Sowa, *Adv. Inorg. Chem.*, 1999, **46**, 173; (*f*) N. R. Champness and M. Schroder, *Curr. Opin. Solid State Mater. Sci.*, 1998, **3**, 419; (*g*) A. J. Blake, N. R. Champness, P. Hubberstey, W. S. Li, M. A. Withersby and M. Schröder, *Coord. Chem. Rev.*, 1999, **183**, 117; (*h*) A. N. Khlobystov, A. J. Blake, N. R. Champness, D. A. Lemenovskii, A. G. Majouga, N. V. Zyk and M. Schröder, *Coord. Chem. Rev.*, 2001, **222**, 155; (*i*) M. Eddaoudi, D. B. Moler, H. L. Li, B. L. Chen, T. M. Reineke, M. O'Keeffe and O. M. Yaghi, *Acc. Chem. Res.*, 2001, **34**, 319; (*j*) T. J. Barton, L. M. Bull, W. G. Klemperer, D. A. Loy, B. McEnaney, M. Misono, P. A. Monson, G. Pez, G. W. Scherer, J. C. Vartuli and O. M. Yaghi, *Chem. Mater.*, 1999, **11**, 2633; (*k*) M. J. Zaworotko, *Chem. Commun.*, 2001, 1; (*l*) B. Moulton and M. J. Zaworotko, *Chem. Rev.*, 2001, **101**, 1629; (*m*) B. Moulton and M. J. Zaworotko, *Curr. Opin. Solid State Mater. Sci.*, 2002, **6**, 117.

2 See, *e.g.*, (*a*) G. B. Gardner, D. Venkataraman, J. S. Moore and S. Lee, *Nature (London)*, 1995, **374**, 792; (*b*) D. Venkataraman, G. B. Gardner, S. Lee and J. S. Moore, *J. Am. Chem. Soc.*, 1995, **117**, 11601; (*c*) C. Janiak, *Angew. Chem., Int. Ed. Engl.*, 1997, **36**, 1431; (*d*) O. M. Yaghi, G. Li and H. Li, *Nature (London)*, 1995, **378**, 703; (*e*) O. M. Yaghi, H. Li, C. Davis, D. Richardson and T. L. Groy, *Acc. Chem. Res.*, 1998, **31**, 474; (*f*) H. Li, M. Eddaoudi, M. O'Keeffe and O. M. Yaghi, *Nature (London)*, 1999, **402**, 276; (*g*) M. Eddaoudi, H. Li and O. M. Yaghi, *J. Am. Chem. Soc.*, 2000, **122**, 1391; (*h*) M. Eddaoudi, J. Kim, N. Rosi, D. Vodak, J. Wachter, M. O'Keeffe and O. M. Yaghi, *Science (Washington, D. C.)*, 2002, **295**, 469; (*i*) S. Noro, S. Kitagawa, M. Kondo and K. Seki, *Angew. Chem. Int. Ed.*, 2000, **39**, 2081; (*j*) S. Noro, R. Kitaura, M. Kondo, S. Kitagawa, T. Ishii, H. Matsuzaka and M. Yamashita, *J. Am. Chem. Soc.*, 2002, **124**, 2568; (*k*) R. Kitaura, K. Seki, G. Akiyama and S. Kitagawa, *Angew. Chem. Int. Ed.*, 2003, **42**, 428; (*l*) M. J. Zaworotko, *Angew. Chem. Int. Ed.*, 2000, **39**, 2113; (*m*) C. J. Kepert, T. J. Prior and M. J. Rosseinsky, *J. Am. Chem. Soc.*, 2001, **123**, 10001.

3 D. Hagrman, R. P. Hammond, R. Haushalter and J. Zubieta, *Chem. Mater.*, 1998, **10**, 2091.

4 L. Carlucci, G. Ciani, D. M. Proserpio and S. Rizzato, *Chem. Commun.*, 2000, 1319.

5 L. Carlucci, G. Ciani, M. Moret, D. M. Proserpio and S. Rizzato, *Angew. Chem., Int. Ed. Engl.*, 2000, **39**, 1506.

6 L. Carlucci, G. Ciani, D. M. Proserpio and S. Rizzato, *J. Chem. Soc., Dalton Trans.*, 2000, 3821.

7 M. Tanner and A. Ludi, *Chimia*, 1980, **34**, 23.

8 G. M. Sheldrick, *SADABS: Siemens Area Detector Absorption Correction Software*, University of Goettingen, Germany, 1996.

9 A. Altomare, M. C. Burla, M. Camalli, G. Cascarano, C. Giacovazzo, A. Guagliardi, A. G. Moliterni, G. Polidori and R. Spagna, *J. Appl. Crystallogr.*, 1999, **32**, 115.

10 G. M. Sheldrick, *SHELX-97*, University of Goettingen, Germany, 1997.

11 L. J. Farrugia, *J. Appl. Crystallogr.*, 1999, **32**, 837.

12 E. Keller, *SCHAKAL99*, University of Freiburg, Germany, 1999.

13 L. Spek, *Acta Crystallogr., Sect. A*, 1990, **A46**, C34.

14 P. Van der Sluis and A. L. Spek, *Acta Crystallogr., Sect A*, 1990, **A46**, 194: The SQUEEZE-Bypass method referred therein is widely used in crystallographic analysis of compounds containing substantial amounts of disordered solvent that cannot be located precisely from diffraction data.

15 M. J. Plater, M. R. St. J. Foreman, T. Gelbrich and M. B. Hursthouse, *Inorg. Chim. Acta*, 2001, **318**, 171.

16 C. V. K. Sharma, R. J. Diaz, A. J. Hessheimer and A. Clearfield, *Cryst. Eng.*, 2000, **3**, 201.

17 D. Hagrman, C. J. Warren, R. C. Haushalter, C. Seip, C. J. O'Connor, R. S. Rarig, Jr., K. M. Johnson III, R. L. LaDuca, Jr. and J. Zubieta, *Chem. Mater.*, 1998, **10**, 3294.

18 D. Hagrman, R. C. Haushalter and J. Zubieta, *Chem. Mater.*, 1998, **10**, 361.

19 $[Cd(pyrazine)(SO_4)]$: Orthorhombic, *Pcma* (55), $a = 6.567(1)$ Å, $b = 7.418(1)$ Å, $c = 13.682(2)$ Å, L. Carlucci, G. Ciani, D. M. Proserpio and S. Rizzato, results to be published. After the submission of this paper we have noticed in the current literature another very recent member of this family of coordination networks, namely $[Cd(bipy)(SO_4)]$ (bipy = 4,4′-bipyridine). This species contains the same type of $[Cd(SO_4)]$ layers as in **2**, but shows a smaller interlayer spacing of 11.85 Å. Y. Xu, W.-H. Bi, X. Li, D.-F. Sun, R. Cao and M.-C. Hong, *Inorg. Chem. Commun.*, 2003, **6**, 495.

20 M. O'Keeffe andB. G. Hyde, *Crystal Structures I: Patterns and Symmetry*, Mineral. Soc. Am., Washington, 1996.

21 We have already discussed these features in detail elsewhere: L. Carlucci, G. Ciani and D. M. Proserpio, *Coord. Chem. Rev.*, accepted.

22 (*a*) S. R. Batten and R. Robson, *Angew. Chem. Int. Ed.*, 1998, **37**, 1461; (*b*) S. R. Batten and R. Robson, in *Molecular Catenanes, Rotaxanes and Knots, A Journey Through the World of Molecular Topology*, ed. J.-P. Sauvage and C. Dietrich-Buchecker, Wiley-VCH, Weinheim, 1999, pp. 77–105; (*c*) S. R. Batten, *CrystEngComm*, 2001, **3**, 67; (*d*) S. R. Batten, *Curr. Opin. Solid State Mater. Sci.*, 2001, **5**, 107.
23 L. Carlucci, G. Ciani and D. M. Proserpio, *New J. Chem.*, 1998, **22**, 1319.
24 C. B. Aakeroy, A. M. Beatty and D. S. Leinen, *Angew. Chem. Int. Ed.*, 1999, **38**, 1815.
25 We know how many difficulties are encountered in the attempt to establish a general topological notation for entangled arrays,[21] and we propose here to adopt the concept of 'density of catenation' specifically for polycatenated systems, *i.e.* those having the peculiar feature that all the constituent motifs have lower dimensionality than that of the overall array. A referee of this paper has suggested to modify our notation according to a more 'conventional' usage in inclined interpenetration for describing the 'degree of interpenetration' that implies to count also the sheet containing the fundamental window, *i.e.* in the present case to assume a symbol of the type (4/6/6). We think, however, that our notation is simpler and more suited for these polycatenated systems in that we must clearly distinguish between the concepts of 'degree of interpenetration' and of 'density of catenation'. The suggested modification [*i.e.* the (n + 1) *criterion*] derives, as an extension, from the former concept, that, in turn, has its origin in the classification of 'interpenetrating networks',[22a] and has the meaning of counting the total number (finite) of distinct nets (as, for instance, in the case of an n-fold diamondoid net). In polycatenated systems we cannot define a 'degree of interpenetration' with the same topological meaning as described above. Indeed, in the inclined interweaving of 2D layers (2D → 3D) there is an infinite number of other motifs interlocked with each single motif, and to simply describe such arrays as 'n-fold interpenetrated networks' seems to us rather inadequate. Also, in the case of parallel interweaving of 2D layers (2D → 3D) we prefer to state, for instance, that a layer is catenated to other two (one 'upper' and one 'lower', with a 'density of catenation' equal to 2) rather than to define the system as 3-fold interpenetrated (that seems rather misleading and can be confused with a real case of a 3-fold interpenetration of three layers located on a common average plane). Different systems with peculiar topologies can need different notations.
26 N. Moliner, C. Munoz, S. Letard, X. Solans, N. Menendez, A. Goujon, F. Varret and J. A. Real, *Inorg. Chem.*, 2000, **39**, 5390.
27 M. Kondo, M. Shimamura, S. Noro, S. Minakoshi, A. Asami, K. Seki and S. Kitagawa, *Chem. Mater.*, 2000, **12**, 1288.